

## **Radiation Controls the Interannual Variability of Evaporation of a Subtropical Lake**

Wei Xiao<sup>1,4</sup>, Zhen Zhang<sup>1</sup>, Wei Wang<sup>3</sup>, Mi Zhang<sup>1</sup>, Qiang Liu<sup>1,5</sup>, Yongbo Hu<sup>1</sup>, Wenjing Huang<sup>1</sup>, Shoudong Liu<sup>1</sup>, Xuhui Lee<sup>2</sup>

<sup>1</sup>Yale-NUIST Center on Atmospheric Environment & Collaborative Innovation Center on Forecast and Evaluation of Meteorological Disasters, Nanjing University of Information Science & Technology, Nanjing, China.

<sup>2</sup>School of Forestry and Environmental Studies, Yale University, New Haven, Connecticut, USA.

<sup>3</sup>Jiangsu Key Laboratory of Agricultural Meteorology, Nanjing University of Information Science & Technology, Nanjing, China

<sup>4</sup>NUIST-Wuxi Research Institute, Wuxi, China

<sup>5</sup>Binjiang College of NUIST, Wuxi, China

Correspondence to : Wei Xiao ([wei.xiao@nuist.edu.cn](mailto:wei.xiao@nuist.edu.cn)), Xuhui Lee ([xuhui.lee@yale.edu](mailto:xuhui.lee@yale.edu))

### **Contents of this file**

Figures S1 to S8

### **Introduction**

Here we provide supporting information for our paper *Radiation Controls the Interannual Variability of Evaporation of a Subtropical Lake*. The supporting information consists of the following items:

- satellite image of Lake Taihu and locations of the land and lake sites (Figure S1);
- temporal variability of the radiation budgets, non-energy variables and latent heat flux, and their relationship (Figures S2 to S4; Table S1 and S2);
- variation of the Priestley-Taylor coefficient and the correlation with meteorological variables (Figures S5 to S7) ;
- annual composition of the Bowen ratio (Figure S8).

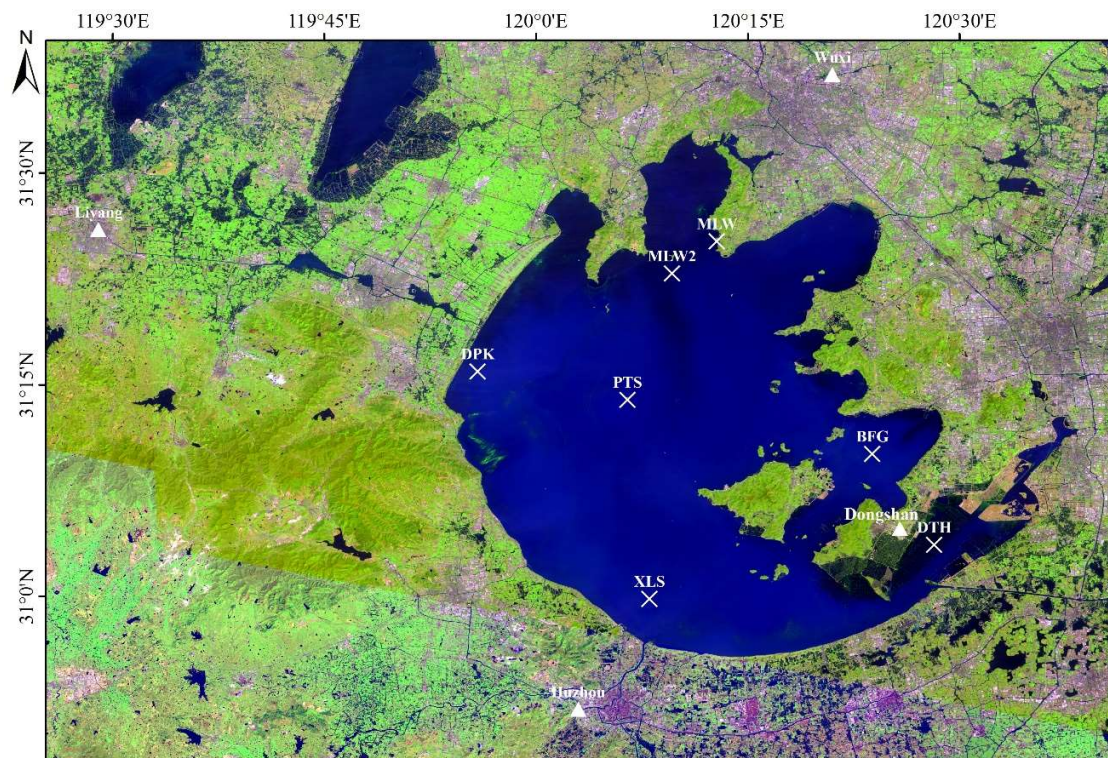


**Figure S1.** Satellite image of Lake Taihu and locations of eddy flux site over the lake (crosses) and over the land (Dongshan), and meteorological station around the lake (triangles).

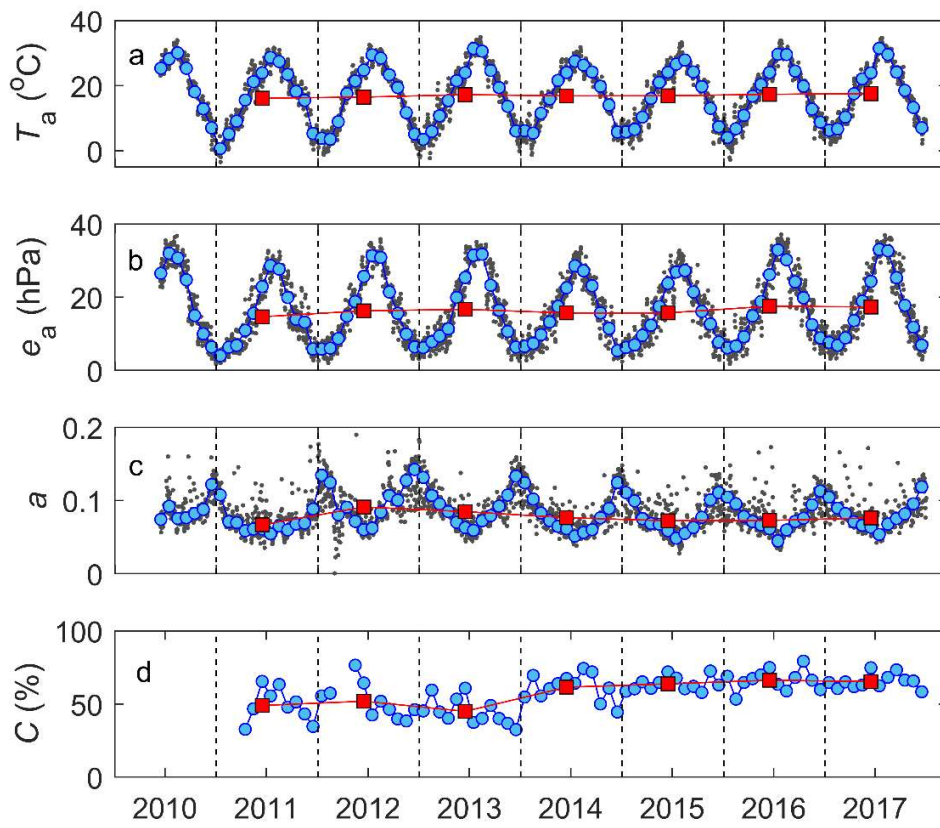


**Figure S2.** Time series of daily (dots), monthly (circles) and annual (squares) air temperature (a), atmospheric vapor pressure (b), surface albedo (c) and cloud cover (d) at Lake Taihu from 2010 to 2017.

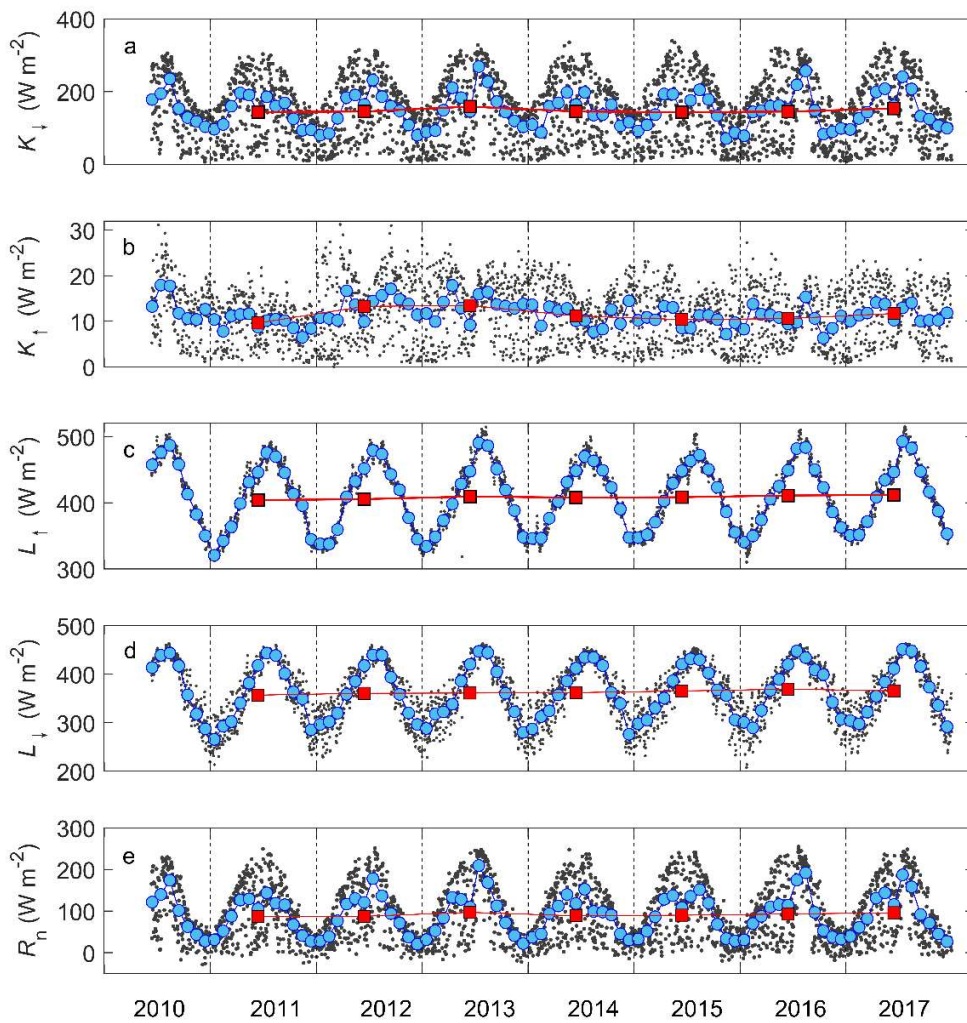


**Figure S3.** Time series of daily (dots), monthly (circles) and annual (squares) solar radiation (a), reflected shortwave radiation (b), outgoing longwave radiation (c), incoming longwave radiation (d) and net radiation (e) at Lake Taihu from 2010 to 2017.

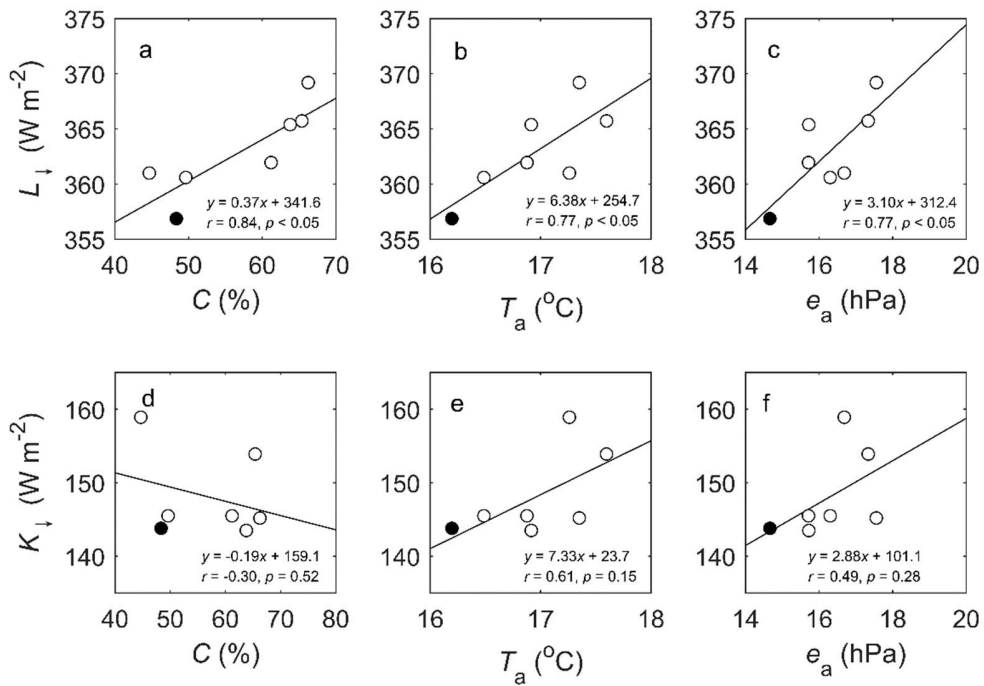


**Figure S4.** Upper panels: Incoming longwave radiation versus cloud cover (a), air temperature (b) and atmospheric vapor pressure (c). Lower panels: Incoming shortwave radiation versus cloud cover (d), air temperature (e) and atmospheric vapor pressure (f). Filled symbols denote observations at MLW in 2011.

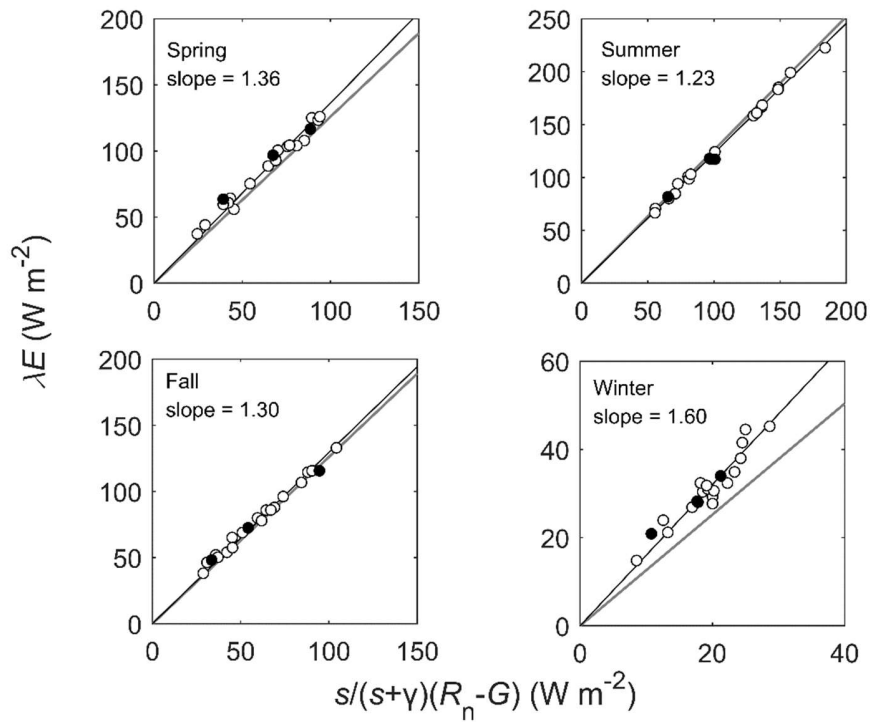


**Figure S5.** Monthly latent heat flux as a function of monthly  $s/(s+\gamma)(R_n - G)$  during spring (March through May), summer (June through August), fall (September through November) and winter (December through next February) from 2011 to 2017. Blue circles: observations; blue lines: linear regression line; black lines: Priestley-Taylor model with the default coefficient of 1.26. Filled symbols denote observations at MLW in 2011.

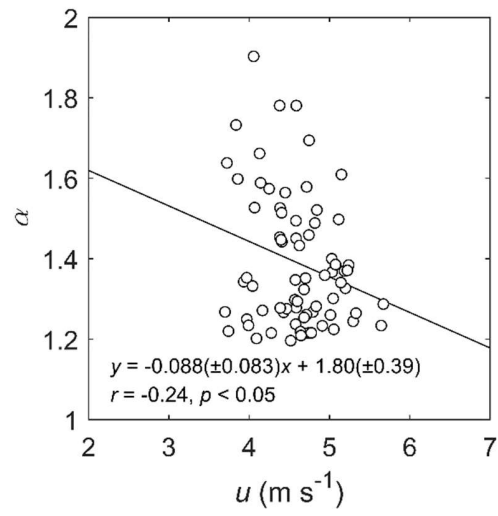


**Figure S6.** The Priestley-Taylor coefficient versus wind speed for each month from 2012 to 2017.



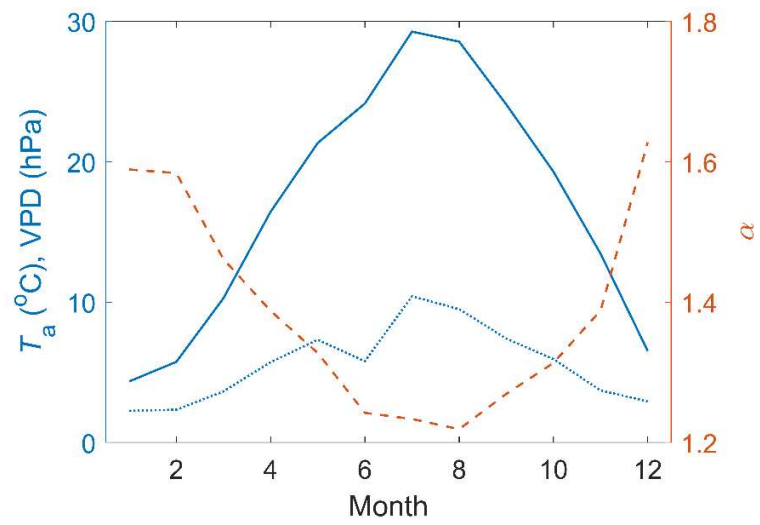


**Figure S7.** Seasonal composite of the Priestley-Taylor coefficient (dashed line), air temperature (solid line) and vapor pressure deficit (VPD, dotted line) from 2011 to 2017.



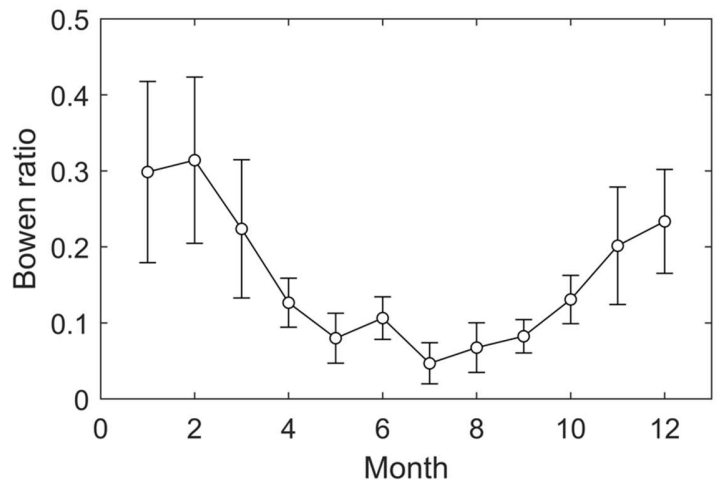


**Figure S8.** Seasonal composite Bowen ratio from 2011 to 2017. Error bars are  $\pm$  one standard deviation.